

Are your MRI contrast agents cost-effective?

Learn more about generic Gadolinium-Based Contrast Agents.



FRESENIUS
KABI

caring for life

AJNR

**Comparison of Dynamic
Contrast-Enhancement Parameters between
Gadobutrol and Gadoterate Meglumine in
Posttreatment Glioma: A Prospective
Intraindividual Study**

J.E. Park, J.Y. Kim, H.S. Kim and W.H. Shim

This information is current as
of April 20, 2024.

AJNR Am J Neuroradiol 2020, 41 (11) 2041-2048

doi: <https://doi.org/10.3174/ajnr.A6792>

<http://www.ajnr.org/content/41/11/2041>

Comparison of Dynamic Contrast-Enhancement Parameters between Gadobutrol and Gadoterate Meglumine in Posttreatment Glioma: A Prospective Intraindividual Study

J.E. Park, J.Y. Kim, H.S. Kim, and W.H. Shim



ABSTRACT

BACKGROUND AND PURPOSE: Differences in molecular properties between one-molar and half-molar gadolinium-based contrast agents are thought to affect parameters obtained from dynamic contrast-enhanced imaging. The aim of our study was to investigate differences in dynamic contrast-enhanced parameters between one-molar nonionic gadobutrol and half-molar ionic gadoterate meglumine in patients with posttreatment glioma.

MATERIALS AND METHODS: This prospective study enrolled 32 patients who underwent 2 20-minute dynamic contrast-enhanced examinations, one with gadobutrol and one with gadoterate meglumine. The model-free parameter of area under the signal intensity curve from 30 to 1100 seconds and the Tofts model-based pharmacokinetic parameters were calculated and compared intraindividually using paired *t* tests. Patients were further divided into progression (*n*=12) and stable (*n*=20) groups, which were compared using Student *t* tests.

RESULTS: Gadobutrol and gadoterate meglumine did not show any significant differences in the area under the signal intensity curve or pharmacokinetic parameters of K^{trans} , V_e , V_p , or K_{ep} (all $P > .05$). Gadobutrol showed a significantly higher mean wash-in rate (0.83 ± 0.64 versus 0.29 ± 0.63 , $P = .013$) and a significantly lower mean washout rate (0.001 ± 0.0001 versus 0.002 ± 0.002 , $P = .02$) than gadoterate meglumine. Trends toward higher area under the curve, K^{trans} , V_e , V_p , wash-in, and washout rates and lower K_{ep} were observed in the progression group in comparison with the treatment-related-change group, regardless of the contrast agent used.

CONCLUSIONS: Model-free and pharmacokinetic parameters did not show any significant differences between the 2 gadolinium-based contrast agents, except for a higher wash-in rate with gadobutrol and a higher washout rate with gadoterate meglumine, supporting the interchangeable use of gadolinium-based contrast agents for dynamic contrast-enhanced imaging in patients with posttreatment glioma.

ABBREVIATIONS: DCE = dynamic contrast-enhanced; CE = contrast-enhanced; GBCA = gadolinium-based contrast agent; IAUC = initial area under the time-to-signal intensity curve; K_{ep} = rate transfer constant; K^{trans} = volume transfer constant; V_e = extravascular-extracellular space per unit volume of tissue; V_p = blood plasma volume per unit volume of tissue; WHO = World Health Organization

In the evaluation of brain tumors on MR imaging, the interpretation of vascular permeability is important because an insufficient blood supply may be related to resistance to chemotherapy or immunotherapy owing to poor and heterogeneous uptake of the therapeutic agents.^{1,2} Dynamic contrast-enhanced (DCE) T1-weighted perfusion MR imaging, which involves the acquisition

of serial images after the administration of a gadolinium-based contrast agent (GBCA), has demonstrated considerable utility for assessing tumor perfusion, vessel permeability, and the volume of the extravascular-extracellular space.³ DCE imaging is widely used for brain tumor imaging and is a useful noninvasive method for monitoring treatment response.⁴⁻⁶

The relationship between the MR signal intensity of a voxel on DCE-MR imaging and the actual concentration of GBCA is

Received May 17, 2020; accepted after revision July 22.

From the Department of Radiology and Research Institute of Radiology (J.E.P., H.S.K., W.H.S.), University of Ulsan College of Medicine, Asan Medical Center, Seoul, Korea; and Department of Radiology (J.Y.K.), Kangbuk Samsung Hospital, Sungkyunkwan University School of Medicine, Seoul, Korea.

Ji Eun Park and Jung Youn Kim contributed equally to this work.

This work was supported by Bayer Korea and by a National Research Foundation of Korea (Ministry of Education) (grant No. NRF-2020RIA2B5B01001707 and NRF-2020RIA2C4001748). The funders had no role in study design, data collection and analysis, decision to publish, or preparation of the manuscript.

Please address correspondence to Ho Sung Kim, MD, PhD, Department of Radiology and Research Institute of Radiology, University of Ulsan College of Medicine, Asan Medical Center, 88 Olympic-ro 43-gil, Songpa-Gu, Seoul 05505, Korea; e-mail: radhskim@gmail.com

Indicates open access to non-subscribers at www.ajnr.org

<http://dx.doi.org/10.3174/ajnr.A6792>

complex, with the measured tissue relaxivity depending on the flip angle, TR, proton density, and precontrast tissue relaxivity.⁷ To date, both half-molar and one-molar GBCAs have been interchangeably used as DCE imaging agents.⁸⁻¹² The GBCA-induced signal enhancement depends on 3 factors:¹³⁻¹⁶ 1) the T1 relaxivity of GBCA, 2) the concentration of GBCA in the ROI, and 3) certain tissue-specific characteristics such as tissue perfusion and extracellular blood volume. Regarding T1 relaxivity, gadobutrol (gadolinium-DO3A-butrol; Gadovist 1.0; Bayer Schering Pharma) is a 1.0 mmol/mL gadolinium chelate agent with approximately 14%–27% higher T1 relaxivity than half-molar GBCAs on 3T MR imaging.^{17,18} The concentration of GBCA in the ROI is determined by the interactions between the contrast agent molecules and tissues, and the non-ionic property of gadobutrol is thought to affect tissue interactions and accumulation rates in a manner different from those of ionic GBCAs.^{13,14} Glioma is rich in negatively-charged glycosaminoglycans,¹⁹⁻²¹ and differences in ionic properties between gadobutrol and gadoterate meglumine (Dotarem; Guerbet), may affect model-free or quantitative pharmacokinetic DCE parameters; however, there is a lack of studies comparing the 2 types of GBCA in DCE imaging, with the 2 types having been used interchangeably to date.

Thus, the aim of our study was to investigate differences in DCE parameters between one-molar nonionic gadobutrol and half-molar ionic gadoterate meglumine in patients with posttreatment glioma, evaluating both model-free and pharmacokinetic quantifications. On a theoretic basis, the higher T1 relaxivity of gadobutrol may provide excellent wash-in characteristics, and its nonionic nature may enable longer retention of the contrast media in tissue with a high negatively-charged content, resulting in higher contrast-related signal in delayed phases of contrast-enhanced imaging in comparison with ionic half-molar agents. We, therefore, used a prolonged DCE acquisition of 20 minutes to ensure sufficient observation of wash-in and washout patterns.

MATERIALS AND METHODS

Study Patients

This prospective study was designed as an intraindividual comparison within a clinical cohort of patients with posttreatment glioma recruited between March 2017 and March 2019 and was approved by the institutional review board of our tertiary hospital (Asan Medical Center, Seoul, South Korea; institutional review board approval No: 2017-0003). Written informed consent was obtained from each patient. A flow diagram of the recruitment of study participants is shown in Fig 1. Patients with brain gliomas who were allocated for contrast-enhanced (CE) T1-weighted imaging and DCE imaging were potentially eligible. The detailed inclusion criteria for the current study were as follows: 1) histopathologic diagnosis of glioma according to the 2016 World Health Organization (WHO) criteria;²² 2) received standard treatment of radiation and chemotherapy (ie, for glioblastoma, concurrent chemoradiotherapy with temozolomide and 6 cycles of adjuvant temozolomide administered after surgical resection or biopsy); 3) a measurable contrast-enhancing lesion of more than 1 × 1 cm on CE-T1WI; 4) no corticosteroid administration within 1 week before DCE imaging; and 5) an image acquisition deemed to be of adequate quality without motion artifacts. The rationale for avoiding

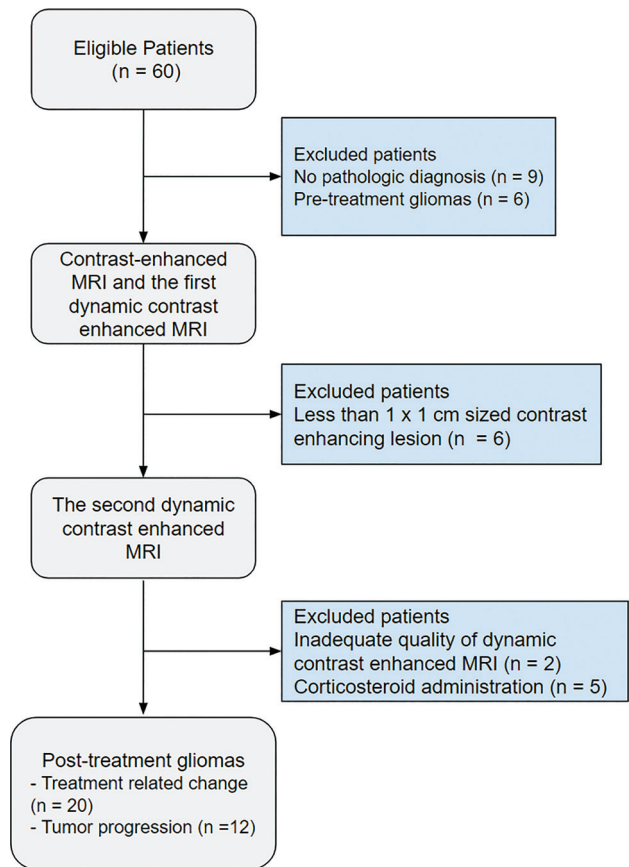


FIG 1. Flow diagram of the participant inclusion process.

a certain period of corticosteroid administration was to avoid the possibility of corticosteroid-induced regression of the tumor.²³

Patients were excluded when there was no pathologic diagnosis ($n = 9$), pre-treatment gliomas ($n = 6$), no visible measurable measurable contrast-enhancing lesion on CE-T1WI ($n = 6$), or when the image quality was deemed inadequate ($n = 2$). Patients who received corticosteroid treatment ($n = 5$) were further excluded. A total of 32 patients (median age, 58 years; age range, 21–76 years; 19 [59.3%] male patients) with posttreatment gliomas were finally included in the study. The clinical characteristics of the patients, including sex, age, extent of surgical treatment for the tumor (gross total resection, partial resection, or biopsy), and pathologic confirmation, were collected from medical records.

MR Imaging Protocol

All MR imaging studies were performed on a 3T unit (Achieva; Philips Healthcare) using an 8-channel head coil. Two DCE imaging examinations were acquired from each patient, with an interval of at least 12 hours between each session. The order of gadobutrol and gadoterate meglumine administration was randomly chosen for each patient. The first session involved acquisition of our dedicated MR imaging protocol for brain tumors, which consisted of T2WI, FLAIR, T1WI, diffusion-weighted imaging, CE-T1WI, and DCE imaging.

DCE imaging was performed using a 3D gradient-echo sequence with 21 slices, with imaging volumes being obtained

after administration of a standard dose of GBCA. Because the one-molar nonionic agent gadobutrol (Gadovist 1.0) is provided at twice the gadolinium concentration of the half-molar ionic gadoterate meglumine (Dotarem), 0.05 mmol (0.1 mL)/kg of body weight (average total volume, 5.8 mL; range, 4–7 mL) of gadobutrol was delivered at a rate of 2 mL/s using an MR imaging-compatible power injector (Spectris; MedRad), whereas 0.1 mmol (0.2 mL)/kg of body weight (average total volume, 13.7 mL; range, 12–15 mL) of gadoterate meglumine was delivered at a rate of 4 mL/s. The temporal resolution was 3.22 seconds, and the contrast material was administered after 10 baseline dynamics. The parameters for the DCE perfusion imaging included section thickness, 4 mm with no gap; TR/TE, 6.4/3.1 ms; flip angle, 15°; FOV, 24 × 24 cm; and matrix, 184 × 186. The total acquisition time for DCE imaging was 18 minutes 40 seconds.

After DCE imaging, CE-T1WI was performed for anatomic reference using a 3D gradient-echo T1-weighted sequence with the following parameters: TR/TE, 9.9/4.6 ms; flip angle, 8°; FOV, 22.4 × 22.4 cm; matrix, 224 × 224; and section thickness, 1 mm with no gap.

Image Registration and Processing

All imaging data were transferred from the MR imaging scanner to an independent computer for quantitative perfusion analysis. For quantitative analysis, contrast-enhancing lesion volumes were segmented on the CE-T1WI using a semiautomated adaptive thresholding technique to select all pixels above a determined threshold value. The resulting segmentation of the entire enhancing tumor was verified by an experienced neuroradiologist (J.E.P., with 7 years of experience in neuro-oncology imaging), who was blinded to the clinical information.

For the DCE imaging, motion correction was performed using rigid-body registration to realign each time point of the time-series. The CE-T1WI was coregistered to the DCE images using an affine transformation with 6 *df* and fourth-degree B-spline interpolation performed using SPM12 (<http://www.fil.ion.ucl.ac.uk/spm/software/spm12>).

The model-free parameters were obtained using Matlab 2019b (MathWorks). The signal intensity was normalized into its percentage change compared with the baseline signal intensity value, and then the initial area under the signal intensity time curve (IAUC) at 30, 100, 200, 300, 400, 500, 600, 700, 800, 900, 1000, and 1100 seconds was calculated for each patient using trapezoidal integration of the normalized signal intensity after the contrast agent arrived in the voxel of interest. Outlier values were automatically removed from the output maps because these can occur due to unstable curve-fitting conditions with a noisy input signal.

The pharmacokinetic parameters were obtained using a dedicated software package (nordicICE; NordicNeuroLab) based on the 2-compartment model proposed by Tofts and Kermode.²⁴ The parameters included volume transfer constant (K^{trans}), rate transfer constant (K_{ep}), blood plasma volume per unit volume of tissue (V_p), and extravascular-extracellular space per unit volume of tissue (V_e). The wash-in rate was calculated as the maximum slope between the time of onset of contrast inflow and the time of peak enhancement on the time-intensity curve. The washout rate was calculated as the negative slope of the late part of the exponential

curve. Each parameter was calculated using a fixed T1 of 1000 ms, because this can contribute to more reliable results and protect the dynamic data from patient movement or inaccurate scaling factors occurring during the DCE imaging acquisition.^{25,26}

The arterial input function was selected by a neuroradiologist (J.Y.K., with 2 years of experience in neuro-oncology imaging), who was blinded to the clinical information of the study subject, using an ROI confined to the vertical portion of the superior sagittal sinus, which avoided problems of feeding veins causing mixed artifacts in the same image section.

Reference Standard for Tumor Progression and Treatment-Related Change

A final diagnosis of tumor progression or treatment-related change was confirmed pathologically in second-look operations when clinically indicated. When second-look operations were not performed, tumor progression on MR imaging was assessed according to the Response Assessment in Neuro-Oncology criteria,²⁷ using serial measures of the product of the 2 largest cross-sectional diameters. The consecutive clinicoradiologic diagnoses were made by consensus between a neuro-oncologist (J.H.K., with 26 years of experience in neuro-oncology practice) and a neuroradiologist (H.S.K., with 21 years of experience in neuro-oncologic imaging) after complete imaging and medical chart review.²⁷

Statistical Analysis

Sample Size. The sample size of our study was determined according to power analysis for paired-means analysis, which was performed using Power Analysis Software (PASS, Version 15.0.7; <https://www.ncss.com/download/pass/updates/pass15/>). We used data on the distribution of the IAUC30 parameter from a previous study,²⁸ which showed mean values of 15.73 ± 2.76 in recurrent glioblastoma and 7.31 ± 3.59 in radiation necrosis, with a meaningful difference between the 2 contrast agents being indicated by a difference of >8.0 . The null hypothesis was that there was no difference in the mean of the paired differences of IAUC30 between the 2 contrast agents. A sample size of 32 would achieve 100% power to detect a mean paired difference of 8.0 with an estimated SD of differences of 7.0 with a significance level (α) of .05 using a 2-sided paired *t* test. This represents significance in a 2-sided *Z*-test ($P < .05$). Thus, the sample size of 32 was sufficient to detect meaningful differences in the 2 contrast agents that would affect the clinical diagnosis of recurrent glioblastoma or radiation necrosis.

DCE parameters were initially assessed for normality using the Shapiro-Wilk test. The DCE parameters were found to be normal and were then expressed as mean \pm SD. Paired *t* tests were used to assess intraindividual differences in the DCE parameters between the 2 GBCAs.

The Student *t* test and χ^2 test were used for comparisons of clinical and demographic characteristics between tumor progression and treatment-related change. Differences in DCE parameters between tumor progression and treatment-related-change groups were assessed using the Student *t* test.

All statistical analyses were performed using SPSS, Version 21 (IBM) and MedCalc, Version 18.2.1 (MedCalc Software). A *P* value $< .05$ was considered statistically significant.

RESULTS

Patient Demographics

Of the 32 study patients, 19 were pathologically confirmed with glioblastoma (WHO grade IV); and 13, with lower-grade astrocytomas (5 with WHO grade II and 8 with grade III; Table 1). There were no differences in age, sex, extent of surgery, and postoperative adjuvant chemotherapy status between the 2 groups.

Comparison of DCE Parameters between Gadobutrol and Gadoterate Meglumine

Table 2 summarizes the comparisons of model-free and pharmacokinetic parameters. When the model-free DCE parameters were compared, gadobutrol showed a trend for a higher rate of relative contrast enhancement compared with gadoterate meglumine, but there was no significant difference in the IAUC 30,

100, 200, 300, 400, 500, 600, 700, 800, 900, 1000, and 1100 seconds (paired *t* test, all $P > .05$).

The pharmacokinetic parameters of K^{trans} , V_e , V_p , and K_{ep} also showed no significant differences between the 2 contrast agents (paired *t* test, all $P > .05$). However, gadobutrol showed a significantly higher mean wash-in rate (0.825 ± 0.644 versus 0.289 ± 0.634 , $P = .013$) and a significantly lower mean washout rate (0.001 ± 0.0001 versus 0.002 ± 0.002 , $P = .02$) than gadoterate meglumine. Figures 2 and 3 show representative cases in patients with tumor progression and treatment-related change, exhibiting differences in wash-in and washout rates.

Subgroup Analysis between Tumor Progression and Treatment-Related Change in DCE Parameters

Table 3 summarizes the comparisons of DCE parameters between the tumor-progression and treatment-related-change groups. The higher wash-in and lower washout rates with gadobutrol compared with gadoterate meglumine were maintained in the tumor-progression and treatment-related-change subgroups, with the higher mean wash-in rate with gadobutrol being especially notable in the treatment-related-change group (0.813 ± 0.521 versus 0.220 ± 0.590 , $P = .002$). The progression group showed trends toward higher areas under the curve, K^{trans} , V_e , V_p , wash-in and washout rates, and lower K_{ep} in comparison with the treatment-related-change group, regardless of the GBCA type, though the differences did not reach statistical significance.

Table 1: Clinical information of the enrolled patients with glioma^a

6-Month Follow-Up	Patients (n = 32)		P Value
	Treatment-Related Change (n = 20)	Tumor Progression (n = 12)	
WHO grade			.71
Grade II	3	2	
Grade III	6	2	
Grade IV	11	8	
No. of male patients	12 (60%)	6 (50%)	.59
Age (yr)	61.5 (36–70)	59.5 (21–69)	.71
Surgical extent (%)			.46
Biopsy or partial resection	14	7	
Gross total resection	6	5	
Postoperative standard radiation therapy or concurrent chemoradiation therapy	19	11	.55

^aData are expressed as the median and range for continuous variables. The χ^2 test was used to test for differences in categorical variables between the 6-month stable and tumor-progression groups.

Table 2: Intraindividual comparison of model-free and pharmacokinetic parameters between gadobutrol and gadoterate meglumine dynamic contrast-enhanced MR imaging^a

DCE Parameter	Gadobutrol	Gadoterate Meglumine	P Value
Model-free method			
IAUC30	3.91 ± 2.38	4.27 ± 2.02	.517
IAUC100	21.50 ± 12.82	23.41 ± 11.28	.530
IAUC200	39.08 ± 23.30	42.53 ± 20.57	.533
IAUC300	56.68 ± 33.77	61.68 ± 29.88	.533
IAUC400	74.25 ± 44.24	80.79 ± 39.17	.534
IAUC500	91.84 ± 54.71	99.91 ± 48.46	.534
IAUC600	109.44 ± 65.19	119.06 ± 57.76	.534
IAUC700	127.04 ± 75.66	138.21 ± 67.07	.535
IAUC800	144.66 ± 86.13	157.37 ± 76.37	.535
IAUC900	166.69 ± 98.74	179.04 ± 83.13	.656
IAUC1000	184.76 ± 109.43	198.43 ± 92.13	.656
IAUC1100	202.85 ± 120.13	217.84 ± 101.13	.657
Pharmacokinetic method			
K^{trans} (min ⁻¹)	0.016 ± 0.009	0.017 ± 0.008	.592
K_{ep} (min ⁻¹)	0.127 ± 0.042	0.132 ± 0.041	.594
V_e (%)	17.797 ± 10.057	17.271 ± 7.436	.813
V_p	1.168 ± 0.674	1.263 ± 0.600	.559
Wash-in rate	0.825 ± 0.644	0.289 ± 0.634	.013
Washout rate	0.0010 ± 0.0008	0.0021 ± 0.0025	.024

^aData area means. *P* values are from paired tests when the variables satisfied normality according to the Shapiro-Wilk test or from Wilcoxon-signed rank tests otherwise.

DISCUSSION

We compared gadobutrol with gadoterate meglumine on an intraindividual basis to investigate whether model-free and pharmacokinetic parameters from DCE imaging were affected by differences between one-molar nonionic gadobutrol and half-molar ionic gadoterate meglumine. Gadobutrol had a significantly higher wash-in rate and a lower washout rate compared with gadoterate meglumine. However, neither the model-free parameters obtained from relative signal change nor the pharmacokinetic parameters of K^{trans} , V_e , V_p , or K_{ep} showed any significant difference between the 2 GBCAs. Both GBCAs showed the same trends of higher leakage parameter values, except for the comparison of K_{ep} between the tumor progression group and the treatment-related-change group, though the 2 GBCAs showed no significant difference

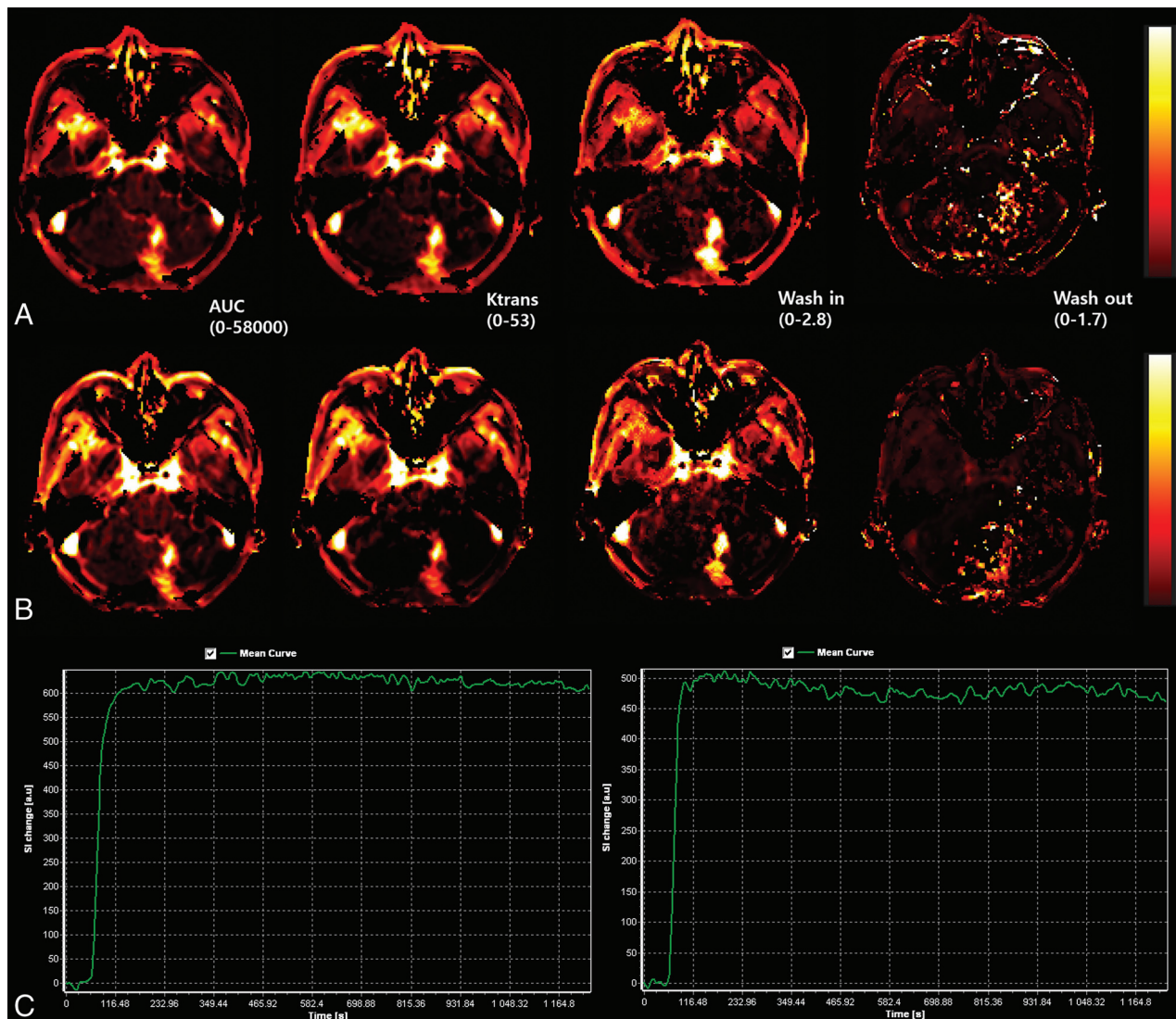


FIG 2. A 62-year-old female patient with posttreatment glioblastoma at 15 weeks after concurrent chemoradiotherapy exhibits a contrast-enhancing mass on DCE imaging with gadobutrol (A, upper row) and gadoterate meglumine (B, lower row). The K^{trans} , IAUC 30, K_{ep} , V_{e} , V_{p} , and dynamic curve show similar patterns and values. Wash-in and washout maps show differences between the 2 gadolinium-based contrast agents. The patient was diagnosed with tumor progression. C, The time-to-signal intensity curves (left: gadobutrol and right: gadoterate meglumine) are shown for both contrast agents. SI indicates signal intensity.

between the 2 groups. Our results support the current notion that one-molar nonionic gadobutrol and half-molar ionic gadoterate meglumine can be used interchangeably for DCE imaging in patients with posttreatment gliomas.

Using pharmacokinetic parameters, previous studies found that treatment-related change demonstrated lower K^{trans} , V_{e} , and V_{p} than tumor progression, especially in glioblastoma.^{29,30} The diagnostic utility of the model-free parameters of IAUC at 30 and 60 seconds was also previously demonstrated.^{28,31-34} Recently, standardization of the DCE image-processing method has been pursued,¹² with a method involving 2-compartment pharmacokinetic modeling with patient-specific baseline T1 maps and a vascular input function taken from the superior sagittal sinus. Nonetheless, GBCA use has not been standardized, and there are only limited reports comparing DCE patterns between one-molar and half-molar gadolinium-based contrast agents.^{16,35-40}

Whereas some authors reported that gadobutrol resulted in an increase in diagnostic accuracy for detecting prostate cancer in comparison with half-molar GBCAs,⁴¹ other studies^{16,42-44} performed on different organs did not show significant diagnostic benefits with gadobutrol. A recent in vitro study comparing gadobutrol and other half-molar GBCAs in various body regions showed significant differences in signal enhancement among body regions.¹⁵ The highest amplitude of signal enhancement was observed in the blood, followed by well-perfused organs such as the spleen, liver, tongue, and prostate, whereas much lower signal intensity was observed in extremity muscle and only minor signal changes were detected in brain tissue, probably attributable to the blood-brain barrier.¹⁵ Our results indicate that it is unlikely that there would be any significant difference between one-molar nonionic gadobutrol and half-molar ionic gadoterate meglumine when they are used to establish clinical diagnoses or management plans in patients with posttreatment glioma. Our study has value in that it performed a direct head-to-head

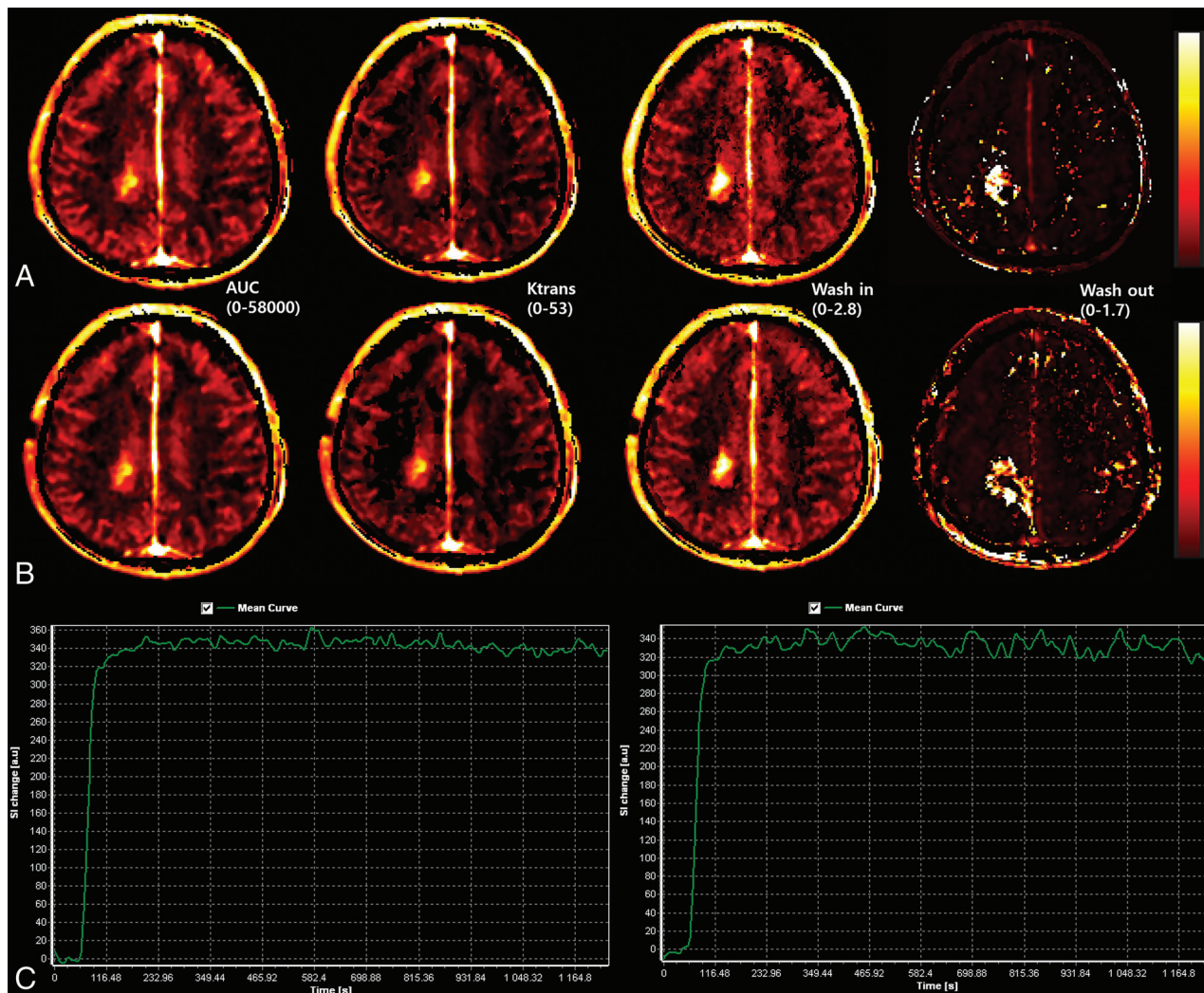


FIG 3. A 55-year-old female patient with posttreatment glioblastoma at 15 weeks after concurrent chemoradiotherapy exhibits a contrast-enhancing mass on DCE imaging with gadobutrol (A, upper row) and gadoterate meglumine (B, lower row). The K^{trans} , IAUC 30, K_{ep} , V_e , V_p , and dynamic curve show similar patterns and values. Wash-in and washout maps show differences between the 2 gadolinium-based contrast agents. The patient was diagnosed with treatment-related change. C, The time-to-signal intensity curves (left: gadobutrol and right: gadoterate meglumine) are shown for both contrast agents. SI indicates signal intensity.

comparison between one- and half-molar GBCA, and our results imply that the 2 GBCA types can be used interchangeably for most of the DCE parameters, thereby supporting the standardization of DCE imaging in patients with posttreatment glioma.

Both gadobutrol and gadoterate meglumine are macrocyclic gadolinium agents and are known to be safer than linear gadolinium agents because of their higher kinetic stability.^{17,45,46} Many studies have shown that contrast agents with higher T1 relaxivity result in stronger contrast enhancement than those with lower T1 relaxivity.^{16,35,36,47} The combined properties of higher gadolinium concentration and T1 relaxivity obtained with gadobutrol could have resulted in a significantly higher wash-in rate calculated by the pharmacokinetic method in comparison with gadoterate meglumine; however, the model-free method with calculation of the IAUC is a robust and simple indicator of tumor vascular characteristics,⁴⁸ and the IAUCs did not show any significant difference between the 2 GBCAs. We, therefore, suggest that the results can be interpreted without having to consider the molarity of the GBCA.

Our finding of a difference in the washout rate is in accord with previous studies in the breast, which demonstrated slower washout of gadobutrol than gadoterate meglumine.^{16,36} The difference might be attributable to the difference in ionic properties between the 2 contrast agents, with the higher washout rate of gadoterate meglumine reflecting its lower accumulation in the extravascular extracellular space compared with gadobutrol. A previous DCE study of cartilage¹⁴ showed that a nonionic neutral agent revealed diffuse contrast enhancement independent of glycosaminoglycan concentration, while a negatively charged ionic agent showed a negative correlation between signal enhancement and the concentration of glycosaminoglycan. This effect was explained by electrostatic repulsion between the ionic contrast agent and the negatively charged glycosaminoglycan-rich extravascular-extracellular space.¹⁴ The extravascular-extracellular space of gliomas is glycosaminoglycan-rich,¹⁹⁻²¹ which may have contributed to the faster washout of the ionic contrast agent compared with the nonionic agent.

Table 3: Intraindividual comparisons of model-free and pharmacokinetic parameters between stable and progression posttreatment glioma groups^a

DCE Parameters	Treatment-Related Change Group			Progression Group			P Value ^{a,b}	P Value+ ^b
	Gadobutrol	Gadoterate Meglumine	P Value	Gadobutrol	Gadoterate Meglumine	P Value		
Model-free method								
IAUC30	3.43 ± 1.59	3.90 ± 1.84	.399	4.69 ± 3.24	4.88 ± 2.25	.870	.15	.34
IAUC100	15.82 ± 7.88	17.91 ± 9.21	.446	20.55 ± 13.69	21.20 ± 9.51	.895	.22	.34
IAUC200	15.80 ± 7.87	17.89 ± 9.20	.446	20.54 ± 13.67	21.18 ± 9.49	.896	.22	.34
IAUC300	15.82 ± 7.88	17.91 ± 9.20	.445	20.56 ± 13.67	21.21 ± 9.50	.894	.22	.34
IAUC400	15.79 ± 7.87	17.88 ± 9.18	.445	20.54 ± 13.66	21.17 ± 9.49	.897	.22	.34
IAUC500	15.81 ± 7.87	17.90 ± 9.19	.445	20.55 ± 13.66	21.18 ± 9.50	.898	.22	.34
IAUC600	15.82 ± 7.87	17.91 ± 9.20	.445	20.57 ± 13.66	21.20 ± 9.50	.897	.22	.34
IAUC700	15.83 ± 7.87	17.92 ± 9.20	.445	20.57 ± 13.67	21.21 ± 9.51	.896	.22	.34
IAUC800	15.83 ± 7.87	17.92 ± 9.20	.445	20.58 ± 13.67	21.21 ± 9.51	.896	.22	.34
IAUC900	16.64 ± 8.11	18.29 ± 9.45	.651	19.78 ± 13.43	20.69 ± 8.71	.859	.51	.54
IAUC1000	16.65 ± 8.11	18.30 ± 9.46	.651	19.79 ± 13.43	20.70 ± 8.72	.858	.51	.54
IAUC1100	16.66 ± 8.11	18.31 ± 9.46	.651	19.79 ± 13.44	20.72 ± 8.73	.857	.51	.54
Pharmacokinetic method								
K^{trans} (min ⁻¹)	0.015 ± 0.007	0.016 ± 0.008	.531	0.017 ± 0.011	0.018 ± 0.007	.921	.45	.66
K_{ep} (min ⁻¹)	0.130 ± 0.041	0.132 ± 0.041	.878	0.121 ± 0.044	0.133 ± 0.044	.528	.58	.95
V_e (%)	16.374 ± 9.615	16.220 ± 6.271	.952	20.169 ± 10.750	19.023 ± 9.085	.780	.31	.31
V_p	1.045 ± 0.508	1.177 ± 0.591	.454	1.374 ± 0.916	1.408 ± 0.611	.915	.20	.29
Wash-in rate	0.813 ± 0.521	0.220 ± 0.590	.002	0.845 ± 0.859	0.404 ± 0.738	.191	.86	.44
Washout rate	0.0009 ± 0.0004	0.0015 ± 0.0016	.107	0.0013 ± 0.0012	0.0031 ± 0.0033	.091	.17	.08

^a Data are means. P values are from paired t-tests.

^b P* values and P+ values are from Student t tests between the treatment-related-change and tumor-progression groups for gadobutrol and gadoterate meglumine, respectively.

Several limitations to this study should be noted. First, because of the small sample size of the prospective cohort, the statistical power of our data, especially in the tumor-progression group, might be limited. Second, although our study result does not suggest any recommendations for altering clinical practice or patient management, it may still be important to standardize the MR imaging contrast agent to ensure accurate comparisons in patients with posttreatment glioma undergoing monitoring with serial follow-up MR imaging, especially considering the different T1 relaxivities and ionic properties of the 2 types of GBCA.

CONCLUSIONS

Both one-molar nonionic gadobutrol and half-molar ionic gadoterate meglumine showed the same trends in model-free and pharmacokinetic parameters, except for a higher wash-in rate with gadobutrol and a higher washout rate with gadoterate meglumine. Therefore, our findings support the current interchangeable use of these 2 GBCAs for DCE imaging in patients with posttreatment glioma.

ACKNOWLEDGMENT

The authors would like to thank Jeong Hoon Kim for his assistance in clinicoradiologic diagnoses.

REFERENCES

- Chung SR, Choi YJ, Kim HS, et al. Tumor vascular permeability pattern is associated with complete response in immunocompetent patients with newly diagnosed primary central nervous system lymphoma: retrospective cohort study. *Medicine (Baltimore)* 2016;95:e2624 [CrossRef Medline](#)

- Jain RK. Delivery of molecular and cellular medicine to solid tumors. *Adv Drug Deliv Rev* 2001;46:149–68 [CrossRef Medline](#)
- Choyke PL, Dwyer AJ, Knopp MV. Functional tumor imaging with dynamic contrast-enhanced magnetic resonance imaging. *J Magn Reson Imaging* 2003;17:509–20 [CrossRef Medline](#)
- Nguyen TB, Cron GO, Mercier JF, et al. Diagnostic accuracy of dynamic contrast-enhanced MR imaging using a phase-derived vascular input function in the preoperative grading of gliomas. *AJNR Am J Neuroradiol* 2012;33:1539–45 [CrossRef Medline](#)
- Mills SJ, Patankar TA, Haroon HA, et al. Do cerebral blood volume and contrast transfer coefficient predict prognosis in human glioma. *AJNR Am J Neuroradiol* 2006;27:853–58 [Medline](#)
- Tofts, PS. T1-weighted DCE imaging concepts: modelling, acquisition and analysis. *Signal* 2010;500(450):400.
- Evelhoch JL. Key factors in the acquisition of contrast kinetic data for oncology. *J Magn Reson Imaging* 1999;10:254–59 [CrossRef Medline](#)
- Lemasson B, Serduc R, Maisin C, et al. Monitoring blood-brain barrier status in a rat model of glioma receiving therapy: dual injection of low-molecular-weight and macromolecular MR contrast media. *Radiology* 2010;257:342–52 [CrossRef Medline](#)
- Larsen VA, Simonsen HJ, Law I, et al. Evaluation of dynamic contrast-enhanced T1-weighted perfusion MRI in the differentiation of tumor recurrence from radiation necrosis. *Neuroradiology* 2013;55:361–69 [CrossRef Medline](#)
- Marine B, Benjamin L, Régine F, et al. Characterization of tumor angiogenesis in rat brain using iron-based vessel size index MRI in combination with gadolinium-based dynamic contrast-enhanced MRI. *J Cereb Blood Flow Metab* 2009;29:1714–26 [CrossRef Medline](#)
- Kickingereder P, Sahn F, Wiestler B, et al. Evaluation of microvascular permeability with dynamic contrast-enhanced MRI for the differentiation of primary CNS lymphoma and glioblastoma: radiologic-pathologic correlation. *AJNR Am J Neuroradiol* 2014;35:1503–08 [CrossRef Medline](#)
- Anzalone N, Castellano A, Cadioli M, et al. Brain gliomas: multicenter standardized assessment of dynamic contrast-enhanced and dynamic susceptibility contrast MR images. *Radiology* 2018;287:933–43 [CrossRef Medline](#)
- Gillis A, Gray M, Burstein D. Relaxivity and diffusion of gadolinium agents in cartilage. *Magn Reson Med* 2002;48:1068–71 [CrossRef Medline](#)

14. Wiener E, Woertler K, Weirich G, et al. **Contrast enhanced cartilage imaging: comparison of ionic and non-ionic contrast agents.** *Eur J Radiol* 2007;63:110–09 [CrossRef Medline](#)
15. Knobloch G, Frenzel T, Pietsch H, et al. **Signal enhancement and enhancement kinetics of gadobutrol, gadoteridol, and gadoterate meglumine in various body regions: a comparative animal study.** *Invest Radiol* 2020;55:367–73 [CrossRef Medline](#)
16. Renz DM, Durmus T, Bottcher J, et al. **Comparison of gadoteric acid and gadobutrol for detection as well as morphologic and dynamic characterization of lesions on breast dynamic contrast-enhanced magnetic resonance imaging.** *Invest Radiol* 2014;49:474–84 [CrossRef Medline](#)
17. Bellin MF, Van Der Molen AJ. **Extracellular gadolinium-based contrast media: an overview.** *Eur J Radiol* 2008;66:160–07 [CrossRef Medline](#)
18. Rohrer M, Bauer H, Mintonovitch J, et al. **Comparison of magnetic properties of MRI contrast media solutions at different magnetic field strengths.** *Invest Radiol* 2005;40:715–24 [CrossRef Medline](#)
19. Bertolotto A, Giordana MT, Magrassi ML, et al. **Glycosaminoglycans (GASS) in human cerebral tumors.** *Acta Neuropathol* 1982;58:115–19 [CrossRef Medline](#)
20. Bertolotto A, Magrassi ML, Orsi L, et al. **Glycosaminoglycan changes in human gliomas: a biochemical study.** *J Neurooncol* 1986;4:43–48 [CrossRef Medline](#)
21. Bourdon MA, Matthews TJ, Pizzo SV, et al. **Immunochemical and biochemical characterization of a glioma-associated extracellular matrix glycoprotein.** *J Cell Biochem* 1985;28:183–95 [CrossRef Medline](#)
22. Louis DN, Perry A, Reifenberger G, et al. **The 2016 World Health Organization Classification of Tumors of the Central Nervous System: a summary.** *Acta Neuropathol* 2016;131:803–20 [CrossRef Medline](#)
23. Cuoco JA, Klein BJ, Busch CM, et al. **Corticosteroid-induced regression of glioblastoma: a radiographic conundrum.** *Front Oncol* 2019;9:1288 [CrossRef Medline](#)
24. Tofts PS, Kermode AG. **Measurement of the blood-brain barrier permeability and leakage space using dynamic MR imaging. 1: fundamental concepts.** *Magn Reson Med* 1991;17:357–67 [CrossRef Medline](#)
25. Haacke EM, Filletti CL, Gattu R, et al. **New algorithm for quantifying vascular changes in dynamic contrast-enhanced MRI independent of absolute T1 values.** *Magn Reson Med* 2007;58:463–72 [CrossRef Medline](#)
26. Jung SC, Yeom JA, Kim JH, et al. **Glioma: Application of histogram analysis of pharmacokinetic parameters from T1-weighted dynamic contrast-enhanced MR imaging to tumor grading.** *AJNR Am J Neuroradiol* 2014;35:1103–10 [CrossRef Medline](#)
27. Wen PY, Macdonald DR, Reardon DA, et al. **Updated response assessment criteria for high-grade gliomas: Response Assessment in Neuro-Oncology working group.** *J Clin Oncol* 2010;28:1963–72 [CrossRef Medline](#)
28. Chung WJ, Kim HS, Kim N, et al. **Recurrent glioblastoma: optimum area under the curve method derived from dynamic contrast-enhanced T1-weighted perfusion MR imaging.** *Radiology* 2013;269:561–68 [CrossRef Medline](#)
29. Yun TJ, Park CK, Kim TM, et al. **Glioblastoma treated with concurrent radiation therapy and temozolomide chemotherapy: differentiation of true progression from pseudoprogression with quantitative dynamic contrast-enhanced MR imaging.** *Radiology* 2015;274:830–40 [CrossRef Medline](#)
30. Thomas AA, Arevalo-Perez J, Kaley T, et al. **Dynamic contrast enhanced T1 MRI perfusion differentiates pseudoprogression from recurrent glioblastoma.** *J Neurooncol* 2015;125:183–90 [CrossRef Medline](#)
31. Yoon RG, Kim HS, Koh MJ, et al. **Differentiation of recurrent glioblastoma from delayed radiation necrosis by using voxel-based multiparametric analysis of MR imaging data.** *Radiology* 2017;285:206–13 [CrossRef Medline](#)
32. Park JE, Kim HS, Goh MJ, et al. **Pseudoprogression in patients with glioblastoma: assessment by using volume-weighted voxel-based multiparametric clustering of MR imaging data in an independent test set.** *Radiology* 2015;275:792–802 [CrossRef Medline](#)
33. Narang J, Jain R, Arbab AS, et al. **Differentiating treatment-induced necrosis from recurrent/progressive brain tumor using nonmodel-based semiquantitative indices derived from dynamic contrast-enhanced T1-weighted MR perfusion.** *Neuro Oncol* 2011;13:1037–46 [CrossRef Medline](#)
34. Hamilton JD, Lin J, Ison C, et al. **Dynamic contrast-enhanced perfusion processing for neuroradiologists: model-dependent analysis may not be necessary for determining recurrent high-grade glioma versus treatment effect.** *AJNR Am J Neuroradiol* 2015;36:686–93 [CrossRef Medline](#)
35. Haneder S, Attenberger UI, Schoenberg SO, et al. **Comparison of 0.5 M gadoterate and 1.0 M gadobutrol in peripheral MRA: a prospective, single-center, randomized, crossover, double-blind study.** *J Magn Reson Imaging* 2012;36:1213–21 [CrossRef Medline](#)
36. Fallenberg EM, Renz DM, Karle B, et al. **Intraindividual, randomized comparison of the macrocyclic contrast agents gadobutrol and gadoterate meglumine in breast magnetic resonance imaging.** *Eur Radiol* 2015;25:837–49 [CrossRef Medline](#)
37. Anzalone N, Scarabino T, Venturi C, et al. **Cerebral neoplastic enhancing lesions: multicenter, randomized, crossover intraindividual comparison between gadobutrol (1.0M) and gadoterate meglumine (0.5M) at 0.1 mmol Gd/kg body weight in a clinical setting.** *Eur J Radiol* 2013;82:139–45 [CrossRef Medline](#)
38. Maravilla KR, San-Juan D, Kim SJ, et al. **Comparison of gadoterate meglumine and gadobutrol in the MRI diagnosis of primary brain tumors: a double-blind randomized controlled intraindividual crossover study (the REMIND study).** *AJNR Am J Neuroradiol* 2017;38:1681–88 [CrossRef Medline](#)
39. Pediconi F, Kubik-Huch R, Chilla B, et al. **Intra-individual randomized comparison of gadobutrol 1.0 M versus gadobenate dimeglumine 0.5 M in patients scheduled for preoperative breast MRI.** *Eur Radiol* 2013;23:84–92 [CrossRef Medline](#)
40. Koenig M, Schulte-Altendorneburg G, Piontek M, et al. **Intra-individual, randomised comparison of the MRI contrast agents gadobutrol versus gadoteridol in patients with primary and secondary brain tumours, evaluated in a blinded read.** *Eur Radiol* 2013;23:3287–95 [CrossRef Medline](#)
41. Hara T, Ogata T, Wada H, et al. **Prostate cancer detection with multiparametric MRI: a comparison of 1 M-concentration gadobutrol with 0.5 m-concentration gadolinium-based contrast agents.** *Curr Urol* 2018;11:201–05 [CrossRef Medline](#)
42. Saake M, Langner S, Schwenke C, et al. **MRI in multiple sclerosis: an intra-individual, randomized and multicentric comparison of gadobutrol with gadoterate meglumine at 3 T.** *Eur Radiol* 2016;26:820–28 [CrossRef Medline](#)
43. Maravilla KR, Smith MP, Vymazal J, et al. **Are there differences between macrocyclic gadolinium contrast agents for brain tumor imaging? Results of a multicenter intraindividual crossover comparison of gadobutrol with gadoteridol (the TRUTH study).** *AJNR Am J Neuroradiol* 2015;36:14–23 [CrossRef Medline](#)
44. Rahsepar AA, Ghasemiesfe A, Suwa K, et al. **Comprehensive evaluation of macroscopic and microscopic myocardial fibrosis by cardiac MR: intra-individual comparison of gadobutrol versus gadoterate meglumine.** *Eur Radiol* 2019;29:4357–67 [CrossRef Medline](#)
45. Frenzel T, Lengersfeld P, Schirmer H, et al. **Stability of gadolinium-based magnetic resonance imaging contrast agents in human serum at 37 degrees C.** *Invest Radiol* 2008;43:817–28 [CrossRef Medline](#)
46. Sieber MA, Lengersfeld P, Frenzel T, et al. **Preclinical investigation to compare different gadolinium-based contrast agents regarding their propensity to release gadolinium in vivo and to trigger nephrogenic systemic fibrosis-like lesions.** *Eur Radiol* 2008;18:2164–73 [CrossRef Medline](#)
47. Attenberger UI, Runge VM, Morelli JN, et al. **Evaluation of gadobutrol, a macrocyclic, nonionic gadolinium chelate in a brain glioma model: comparison with gadoterate meglumine and gadopentetate dimeglumine at 1.5 T, combined with an assessment of field strength dependence, specifically 1.5 versus 3 T.** *J Magn Reson Imaging* 2010;31:549–55 [CrossRef Medline](#)
48. Evelhoch JL, LoRusso PM, He Z, et al. **Magnetic resonance imaging measurements of the response of murine and human tumors to the vascular-targeting agent ZD6126.** *Clin Cancer Res* 2004;10:3650–57 [CrossRef](#)